Dalton Transactions

PAPER

Cite this: *Dalton Trans.*, 2019, **48**, 989

Benzoic acid as a selector–modulator in the synthesis of MIL-88B(Cr) and nano-MIL-101(Cr)†

Ling Yang,‡[a] Tian Zhao, *‡[a] Ishtvan Boldog, *[b] Christoph Janiak,[b] Xiao-Yu Yang,[c] Qiang Li,[a] Yan-Jia Zhou,[a] Yong Xia,[a] Deng-Wang Lai[a] and Yue-Jun Liu*[a]

Received 19th October 2018,
Accepted 12th December 2018

DOI: 10.1039/c8dt04186e

rsc.li/dalton

The concentration of benzoic acid was found to exercise efficient control over the formation of either MIL-101(Cr) or MIL-88B(Cr) under otherwise similar hydrothermal synthetic conditions. Nanocrystals of MIL-101(Cr) with ~100 nm average size and excellent S_{BET} = 3467 m^2 g^{-1} are obtained at lower concentrations of benzoic acid, while at higher concentrations the microparticulated MIL-88B(Cr) product is formed. Hereby a new efficient synthetic method towards the elusive MIL-88B(Cr), yet reported only once without synthetic details, is proposed. The obtained MIL-88B(Cr) has an interesting and potentially valuable property of retaining its high-volume form (V_{cell} ~ 2000 Å^3) after thermal activation. The degassing of MIL-88B(Cr) in a vacuum at 250 °C yields a porous material with a S_{BET} area of 1136 m^2 g^{-1}, which is around the theoretical maximum. The transition to the denser 'closed' form (V_{cell} ~ 1500 Å^3) occurs only at 350 °C, when all of the benzoate/benzoic acid, hindering the process, is removed.

Introduction

Metal–organic frameworks (MOFs) are porous crystalline coordination networks consisting of metal ions or their clusters interconnected by organic ligands.[1,2] Over the last few years, they have received keen attention[3,4] due to their high porosity, suggesting their significant potential in applications such as gas storage,[5,6] separation,[7,8] catalysis,[9,10] heat transformation,[11] drug delivery[12] and others. Advanced control over the properties of MOF materials is important for potential applications such as luminescence sensors,[13] selective gas adsorption,[14] storage and delivery of small molecules, including drug delivery.[15] The crystal size and morphology of MOF materials could have a crucial influence and should be taken into account.[16–18]

M(III) terephthalates (M = Cr, Fe, Al, V, Mn, In in decreasing order of importance as well as some others) together with terephthalate derivatives and elongated terephthalate analogues form a particularly important sub-class of MOFs. The four best known porous M(III) terephthalates (and terephthalate analogues) are MIL-47/MIL-53, MIL-88, MIL-100 and MIL-101. They are among the most recognized MOF types, especially regarding potential uses. With the exception of MIL-47/MIL-53, based on a 1D-ribbon secondary building unit (SBU), the others are based on a $\{M_3OX(ROO)_6(L^T)_2\}$ triangular-prismatic SBU (X = OH^-, F^-; L^T = H_2O or other terminal solvent–ligands) and hence are polymorphs with the same molecular formula of $[M_3OX(L)_3(L^T)_2]$·*Guests*, differing only in the nature and number of guest molecules. These compounds also often have overlapping conditions of their formation (concomitant polymorphism). In the particular case of V-compounds, the stepwise conversion of MIL-101, MIL-88 and MIL-47 is possible upon heating.[19] In most of the other M(III) cases, the variation of the solvent (typically H_2O or DMF) and/or temperature is enough for the synthesis of at least two compound types in pure forms. High-throughput methods[20] are especially helpful for establishing the optimal conditions. Cr-compounds are an exception: their chemical inertness demands high synthetic temperatures and water is mostly the only viable synthetic medium.

MIL-101 and MIL-88, which are in the focus of our interest, are two unique MOF types. MIL-101 type with an **MTN-e** topology is practically known only as a chromium and vanadium compound with a terephthalate ligand (2,6-naphthalenedicarboxylate analogue was also reported,[21] but its further mentioning is very limited). MIL-101(Cr)[22,23] has outstanding thermal, but particularly chemical robustness,[24–26] arguably one of the

[a]*Key Laboratory of Advanced Packaging Materials and Technology of Hunan Province, School of Packaging and Materials Engineering, Hunan University of Technology, Zhuzhou, 412007, China. E-mail: tian_zhao@hut.edu.cn, yjliu_2005@126.com*

[b]*Institut für Anorganische Chemie und Strukturchemie, Universität Düsseldorf, Universitätsstr. 1, D-40225 Düsseldorf, Germany. E-mail: ishtvan.boldog@gmail.com*

[c]*State Key Laboratory of Advanced Technology for Material Synthesis and Processing, Wuhan University of Technology, Luoshi Road 122, Wuhan 430070, China*

†Electronic supplementary information (ESI) available. See DOI: 10.1039/c8dt04186e

‡These authors contributed equally to this experimental work.

best among all easily accessible MOFs, due to the kinetic stability of the Cr(III) compounds. For example, MIL-101(Cr) could be directly nitrated by a mixture of nitrous and sulfuric acid to form NO_2-MIL-101(Cr).[27] The porosity characteristics of MIL-101(Cr) are also remarkable. The compound features large mesoporous cage cavities with accessible pore diameters of 29 Å and 34 Å, and pore aperture windows of approx. 12 × 12 Å and 16 × 14.7 Å respectively (Fig. S1 in the ESI†) and a BET surface area of ~4000 $m^2\ g^{-1}$.[22] As a result, MIL-101(Cr) could adsorb 1.4 $g\ g^{-1}$ of water[28] or ~1.37 $g\ g^{-1}$ of a much larger ibuprofen drug molecule,[29] values which are arguably unmatched among physisorbents. The combination of high loading and stability is unparalleled, which attracts unflinching attention and stimulates work on further improvement of its properties. One of the evident possibilities is to synthesize MIL-101 in nanoparticulated form, which increases the adsorption kinetics, enhances the sorption selectivity,[30] and broadens the application opportunities.[31,32]

The MIL-88 type has an **acs** net topology, and its realization was reported for Fe, V, Cr, $Ni^{III/II}$ and some other metals, as well as for a number of terephthalate derivatives/analogues, however almost exclusively with iron. MIL-88 is also remarkable for its unparalleled capability to swell/'breathe', to an extent of 270% in MIL-88C(Fe) with 2,6-naphthalenedicarboxylate as a ligand.[33] Deflection of the ·[··M···O–C–O···M··]· moiety from planar conformation *via* hinge movement through the O···O axle with a simultaneous turn of the carboxylate with respect to the benzene ring of the terephthalate ligands secures a possibility of structure extension along the main axis of the structure (Fig. S2 in the ESI†). The swelling is induced primarily by the introduction of guest molecules, which coordinate to the metal atoms of the framework. This extreme swelling ability, unheard of for zeolites, made the MIL-88 compound a target of scrutiny with regard to adsorption separation/enrichment,[34] sensing/analytical determination,[35–37] drug delivery,[38,39] and catalysis.[40,41]

Nevertheless, among all possible MIL-88 realizations with different trivalent metals and their mixtures, only the iron compounds are the ones that are widely employed in application-oriented research. The MIL-88B(Cr), where 'B' denotes a generally accepted *ad hoc* convention for a terephthalate-based compound, is mentioned in a few early publications;[42,43] however, it is enigmatically absent from the subsequent literature. Moreover, the only early original paper by Surblé *et al.*,[43] which claims its synthesis, does not contain experimental details, which is seemingly just an inadvertent, but impactful, omission. In any case, the reported molecular formula evidences the use of pyridine for that synthesis (pyridine is also known as one of the most potent swelling agents for MIL-88 (Fe)).[33] Thus, while it could be considered that the synthetic conditions of MIL-88(Cr) are approximately known, the practical absence of the compound's mentioning in the literature suggests the exigence for a simple reproducible synthetic method, desirably without the use of the toxic pyridine. The lack of information on MIL-88(Cr) was very recently observed by Tanasaro *et al.* who finally made some progress in this direction and reported mixed metal MIL-88(Cr, Fe) compounds with chromium as a dominant metal constituent[44] (this work could be viewed as a continuation of a well-formed sub-area of mixed metal MIL-88 compounds[45,46]). The presence of Fe is crucial, with >25% of iron content in the reaction mixture necessary to induce the formation of the mixed-metal MIL-88 product. However, genuinely pure MIL-88(Cr) compounds are not accessible by this method. The potential interest in MIL-88 (Cr) roots in its high chemical stability, general for chromium compounds, which would allow the use of the compound in a much broader condition range.

Research studies on the influence of different modulators on the porosity and particle morphology of MIL-101 (where the most efficient and once nearly mandatory modulator being the toxic hydrofluoric acid) and MIL-88 materials are relatively numerous. For instance, sodium acetate and hydrofluoric acid were employed to assist the synthesis of hierarchically mesostructured MIL-101(Cr).[47] Weakly alkaline potassium/lithium acetate was used as a mediator to obtain high-quality MIL-101(Cr) with high-surface areas (a BET surface area of up to 3400 $m^2\ g^{-1}$).[48] Recently, we have reported the improved MIL-101(Cr) synthesis method with nitric acid[49] and acetic acid,[50] with the effect of the former in the improvement of the yield (>80%) and processability with the retention of high surface areas, while the latter allows a decrease of the temperature of the synthesis and/or yield nano-sized MIL-101(Cr) with an average particle diameter of approx. 90 nm. On the other hand, there are reports on the influence of acetic acid,[51] (4-trifluoromethyl)cyclohexanecarboxylic acid,[52] polyvinylpyrrolidone[53] and sodium hydroxide (in the latter case, purely *via* pH control)[54] on the size and morphology of different MIL-88(Fe) compounds, which could suggest similar effects for MIL-88B(Cr) (direct analogues are not possible, though, as the synthetic conditions are quite different).

In this publication, we report the interesting role of benzoic acid as a selector between the formation of nanoparticulated MIL-101(Cr) and microparticulated MIL-88B(Cr), thus providing also a simple synthetic approach towards the latter rarely mentioned compound.

Results and discussion

Aiming to research the influence of benzoic acid as a modulator on the formation of MIL-101(Cr) with the primary focus on the size and morphology of the particles constituting the product, a series of experiments using varying amounts of benzoic acid as the modulator were conducted. During the experimentation, we found that with a particular concentration of benzoic acid (HBC) corresponding to a 1 : 1 : 5 ratio for Cr : H_2BDC : HBC, a mixture of MIL-101(Cr) and MIL-88B(Cr) was formed. Further refinement of the conditions has shown that with higher amounts of benzoic acid at about a 1 : 1 : 10 ratio, the formation of practically only the MIL-88B(Cr) took place. Intrigued by this observation, a more in-depth study was undertaken.

In order to understand the effects specific to benzoic acid as a modulator, we avoided the use of any co-modulators, such as hydrofluoric acid. A certain problem was to remove completely the terephthalic and benzoic acids residing in the pores for further appropriate characterization, including the correct estimation of the product yield. Further complications were posed by the formation of phase mixtures, with comparable ratios in some cases. The determination of the yield was performed on a carefully washed sample, which was dried in air until a constant weight was obtained, assuming equilibrium water content in the product. For MIL-101, the reasonably good approximation is the formerly established formula of $[Cr_3(O)(OH)(BDC)_3(H_2O)_2]\cdot 25H_2O$.[49]

The reaction was carried out using 1, 3, 5, 8 and 10 equivalents of the benzoic acid additive and the isolated products are designated respectively as HBC-1, HBC-3, HBC-5, HBC-8 and HBC-10. The sample without the additive is named HBC-0. All these experiments were carried out on 3.0 mmol of both chromium(III) nitrate nonahydrate and terephthalic acid in a PTFE-lined autoclave at 220 °C for 8 hours followed by thorough washing with dimethylformamide and ethanol.

Scanning electron microscopy, SEM (Fig. 1), showed the change of the particle size and their morphology depending on the concentration of the benzoic acid used. HBC-0, HBC-1 and HBC-3 samples chiefly exhibit particles with an octahedral morphology, characteristic of MIL-101(Cr), while the increase of the concentration of benzoic acid causes a decrease of the average crystal size. Their distribution could be well described as a Gaussian distribution and the respective parameters are given in Fig. S4† and Table 1. Sample HBC-0, prepared without an additive, possessed the largest particle size with the maximum distribution, approximating the average size, at around 387 nm. When 1 equivalent of benzoic acid was added to the synthetic medium (HBC-1), the average size decreased to 156 nm. When the amount of benzoic acid was increased to 3 equivalents, the resulting MIL-101(Cr) (HBC-3) with an average particle diameter of approx. 100 nm was obtained (further SEM images are shown in Fig. S3 in the ESI†). The effect of the decrease of crystal sizes is similar in nature to the phenomenon observed previously by us when acetic acid was used as a modulator.[50]

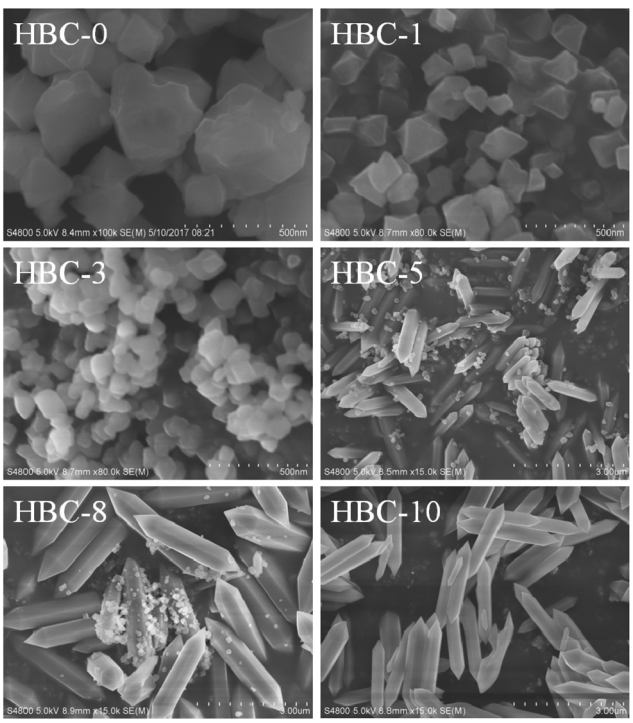

Fig. 1 SEM images of the prepared samples. For HBC-0, HBC-1 and HBC-3, the scale bar is 500 nm, while for HBC-5, HBC-8 and HBC-10 the scale bar is 3 μm.

Interestingly, the increase of benzoic acid concentration to nearly double or more, which corresponds to the use of 5, 8 or 10 equivalents in the performed experiments, caused the formation of lesser amounts or no MIL-101(Cr). Instead, sharp-tipped rod-like crystals with sizes in the micrometer range were observed by SEM and subsequently confirmed to be MIL-88B(Cr). HBC-5 still contains a significant amount of nano-sized MIL-101(Cr) together with the new microcrystalline phase (the enlarged SEM micrographs of HBC-5, HBC-8 and HBC-10 are given in Fig. S3†). Thereby an interesting effect of a relatively sharp change of crystallization outcome depending on the concentration of the benzoic acid was observed, with a higher concentration favouring the MIL-88B(Cr) form. Indeed, for HBC-8, the content of nano-MIL-101(Cr) decreases further and the rod-like MIL-88B(Cr) became dominant, while for HBC-10 only the micrometer-sized rod-like crystals of MIL-88B (Cr) were observed. The nano-MIL-101(Cr) and MIL-88B(Cr) were also characterized by transmission electron microscopy (TEM) and the micrographs correspond well to the expected morphologies (Fig. S5†). The powder X-ray diffractograms, PXRDs, of the HBC-0, HBC-1 and HBC-3 samples corresponding to the lower concentrations of benzoic acid match well with the simulated patterns for MIL-101(Cr), generated using the known crystal structure[22] using the program MERCURY[55] (Fig. 2a). For the samples prepared using higher concentrations of benzoic acid, namely HBC-5, HBC-8, and HBC-10, the patterns reflect the increasing content of the MIL-88B(Cr) phase. Thus, the PXRD of HBC-5 exhibits a comparable ratio of MIL-101(Cr) and MIL-88B(Cr), while in the case of HBC-8 and HBC-10 the relative amounts of MIL-101 (Cr) are small and negligible, respectively, so that the PXRD evidences the presence of MIL-88B only (Fig. 2b; see also an additional comparison of the PXRD patterns of HBC-3 and HBC-10 and of the simulated MIL-101 and MIL-88B compounds in Fig. S6, ESI†). The low-angle region of the PXRD patterns also gave an additional confirmation that the HBC-10 compound is practically pure (please see Fig. S6c, ESI†).

Nitrogen gas sorption isotherms of all benzoic acid-modulated products are shown in Fig. 3, and the porosity results are summarized in Table 1. HBC-0 and HBC-3 samples showed the typical I(b)-type adsorption isotherms[56] as reported in the literature for MIL-101(Cr)[22] (Fig. 3a). Sample HBC-3 with the smallest nano-particle size expectedly possesses the highest

Table 1 Particle size, surface area and pore volume for chromium-benzenedicarboxylate with various amounts of benzoic acid (HBC) as the additive

Benzoic acid (HBC)-(equivalents)[a]	MOF type	Particle size[b] (nm)	S_{BET}[c] ($m^2\ g^{-1}$)	$S_{Langmuir}$ ($m^2\ g^{-1}$)	V_{pore}[d] ($cm^3\ g^{-1}$)	N_2 uptake[d] ($cm^3\ g^{-1}$)
HBC-0	MIL-101	387 (28)	2804	4056	1.92	1243
HBC-1	MIL-101	156 (17)	3254	4949	2.32	1502
HBC-3	MIL-101	100 (12)	3467	4902	2.38	1540
HBC-5	MIL-101/MIL-88	—	2063/126[e]	3093/189[e]	1.86/0.43[e]	1303/107[e]
HBC-8	MIL-101/MIL-88	—	1274/70[e]	1963/99[e]	1.27/0.08[e]	825/50[e]
HBC-10	MIL-88	—	1136/60[e]	1739/77[e]	0.66/0.08[e]	743/49[e]

[a] Benzoic acid equivalents with respect to chromium and H_2BDC. The molar Cr : BDC ratio is always 1 : 1. [b] The average particle size is analysed using a Gaussian distribution model and the estimated standard deviations are given in parentheses. HBC-8 and HBC-10 consist primarily of micrometer-sized rod-shaped MIL-88B(Cr) crystals (this is the typical size resulting from a conventional synthesis without a modulator; hence, the average particle sizes were not estimated). [c] S_{BET} is calculated using data points in the range of $0.05 < P/P_0 < 0.2$ from N_2 sorption isotherms at 77 K with an estimated standard deviation of ±50 $m^2\ g^{-1}$. [d] Calculated from N_2 sorption isotherms at 77 K ($P/P_0 = 0.99$) for pores with ≤ 20 nm diameters. [e] The results are given as value(T_1)/value(T_2), where T_1 and T_2 = 250 °C and 350 °C are the two used degassing temperatures.

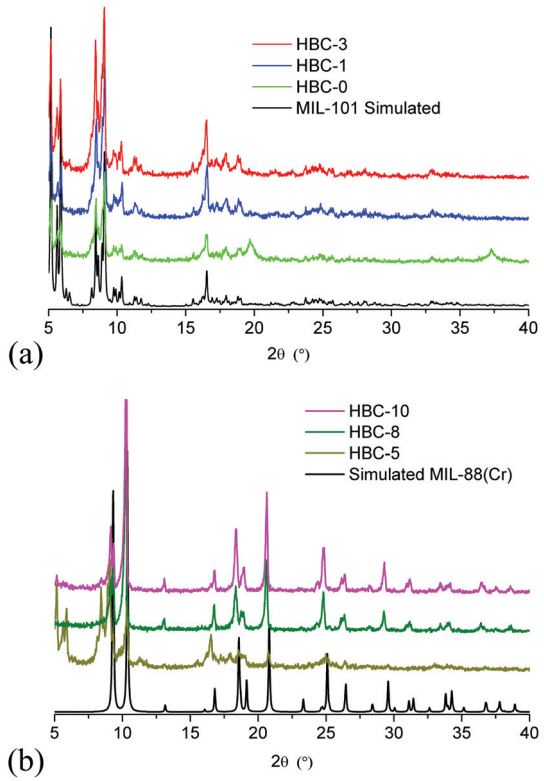

Fig. 2 (a) The PXRD patterns of B-0, B-1, and B-3 samples compared with the simulated pattern of MIL-101(Cr) (CSD-refcode: OCUNAK).[22] (b) The PXRD patterns of B-5, B-8, and B-10 samples compared with the simulated pattern of the 'open' high-volume structure of MIL-88B(Cr) synthesized in the presence of pyridine (CSD-refcode: YEDKOI).[43] See also Fig S8.†

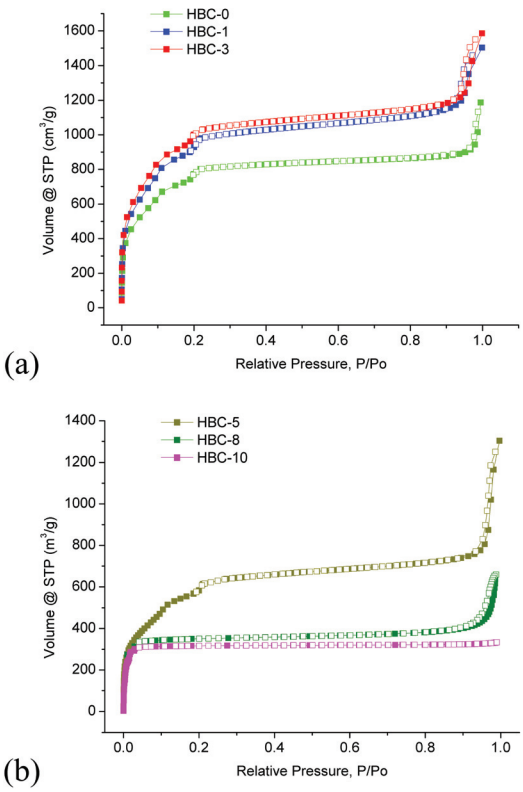

Fig. 3 (a) N_2 adsorption–desorption isotherms for the HBC-0, HBC-1 and HBC-3 samples. (b) N_2 adsorption–desorption isotherms for the HBC-5, HBC-8 and HBC-10 samples after degassing in a vacuum at 250 °C; filled symbols stand for adsorption and empty symbols for desorption.

Brunauer–Emmett–Teller (BET) surface area of 3467 $m^2\ g^{-1}$ and the total pore volume of 2.38 $cm^3\ g^{-1}$. Nevertheless, with a further increase of the concentration of benzoic acid in the reaction medium, the BET surface area and the total pore volume decreased dramatically, due to the formation of MIL-88B(Cr) (Table 1). HBC-5 still largely consists of MIL-101(Cr), which is reflected by the shape of the adsorption isotherm with a small step at P/P_0 = ~0.2 characteristic of MIL-101(Cr); however, the porosity of 2063 $m^2\ g^{-1}$ is much lower. Samples HBC-8 and HBC-10 consist mainly of MIL-88B(Cr) and the respective adsorption isotherms were of I(a)-type,[56] characteristic of that type of material, without any

features typical of mesoporosity (note the degassing temperature of 250 °C for HBC-5–10; Fig. 3b).

The observation of porous MIL-88B(Cr) was highly unexpected, as it is well-known that the dried MIL-88B(Cr) adopts the low-volume form (V_{cell} ~ 1500 Å), which is practically non-porous. In a representative row of known phenyl-functionalized MIL-88B(Fe)-R_n compounds, only two specimens demonstrate significant porosity: R, n = CH_3, 4 with S_{BET} = 1216 and CF_3, 2 with 330 m^2 g^{-1}.[57] The reason for such unusual behavior of the obtained MIL-88B(Cr) evidently roots in the presence of residual amounts of benzoate/benzoic acid in the pores (the assumption regarding the differences stemming from the Fe^{III} *vs.* Cr^{III} dissimilarity is theoretically possible, but implausible in this case, as the framework flexibility was documented for MIL-88A(Cr)).[41] Indeed, it was firmly established that the solvent-induced swelling of MIL-88B(Cr) is associated with the presence of polar solvent molecules, which are capable of coordinating to the terminal positions of the $\{M_3^{III}O(OH)(RCOO)_6(L^T)_2\}$ cluster, with such L^T-s as pyridine or dimethylformamide ensuring the highest swelling ratios.[33,57] Benzoic acid perfectly fits for such a role, while the benzoate anion could, seemingly, act as a substitute for the terminal OH^- ligand as well. Complete removal of benzoic acid and particularly the coordinated benzoate anion should foreseeably be achieved only under quite harsh conditions. It turned out that degassing at 350 °C in a vacuum indeed causes a transition to the MIL-88B(Cr)-'closed' phase as witnessed by both PXRD (Fig. S8†) and N_2 gas adsorption (Table 1, Fig. S7 in the ESI†). According to the PXRD pattern, which satisfactorily matches the expected 'closed' form, a noticeable, but not drastic, decrease of crystallinity occurs. The surface areas drop to S_{BET} < ~70 m^2 g^{-1}, which might have a contribution both from some residual 'opened' and trace amounts of MIL-101(Cr) below the detection capability of the PXRD measurement.

The S_{BET} = 1136 m^2 g^{-1} of the purest MIL-88(Cr) sample somewhat exceeds the theoretical maximum. Our geometric Connolly surface area calculation[58] for a 3.68 Å spherical probe on the YEDKOI[43] structure with guest molecules removed gave values of 544 m^2 g^{-1} and 1092 m^2 g^{-1} areas for structures with hexa- and pentacoordinated Cr atoms, respectively, with O atoms as terminal ligands in the former case. The expected ratio of such atoms for a thoroughly degassed structure is 1 : 2, and the interpolated surface area is ~910 m^2 g^{-1}. The mild discrepancy could be explained both by the already-mentioned trace impurities of MIL-101(Cr) and, possibly, by slightly larger cell parameters of the obtained MIL-88B(Cr). Slight overestimation might also come from using the standard P/P_0 = 0.05–0.2 interval, which is not precise for MOFs with small pores.[59] On the other hand, the observed surface area clearly indicates that the amount of the benzoate/benzoic acid in the pores is very small. It seems very plausible that the predominant form is the coordinated benzoate, which is very hard to eliminate, especially in the absence of water. Moreover, it is expectedly enough to have a far less than one benzoate per $\{M_3^{III}O\}$ moiety in order to prevent a transition, which is concerted for all the clusters (*i.e.* x is close to zero in the $[M_3^{III}O(OH)_{1-x}(OOCPh)_x(RCOO)_6]$ averaged cluster formula).

A thermal gravimetric analysis (TGA) study was performed on HBC-3 and HBC-10 (Fig. 4, the TG curves of the other samples are presented in Fig. S9 in the ESI;† the as-synthesized samples had been stored in ambient air for several days, thus equilibrating their water content, and were measured without further treatment). The TG curve of HBC-3 showed three main weight-loss steps between room temperature and 600 °C. As previously observed for MIL-101(Cr), the first step, r.t.–~120 °C, corresponds to the removal of the water molecules residing freely in the pores of the compound. The second step, 120–~350 °C, corresponds to the removal of the coordinated water molecules, the residual H_2BDC molecules and, at least partially, the terminal benzoates in the form of benzoic acid. The third step, occurring from 350 °C to 550 °C, corresponds to complete destruction of the framework, whose collapse starts at the beginning of the given temperature range, with possible concomitant ligand decarboxylation. The water content of MIL-101(Cr) depends on the method of sample preparation, in our case from the humidity of the air, and could vary from 10% to 20%.[22] The microcrystalline HBC-10 (MIL-88B(Cr)) is more thermally stable than the synthesized MIL-101(Cr) materials consisting of smaller particles, which is reflected by the TG curve (stability to approx. T_{max} of 350 °C *vs.* ~300 °C), but otherwise the general weight loss steps are similar.[22,43] The final decomposition associated with the decarboxylation of the terephthalic acid accelerates at around 350 °C, where the mass loss starts to correspond primarily to the decomposition of the framework, including the ligand's decarboxylation, and the removal of the terminal benzoates. The latter contribution cannot be established precisely, using the not well-resolved TGA curve. If the relatively straight 330–380 °C segment is associated with the benzoates, the respective 3.7% loss would translate to x = ~0.25 (see the cluster formula above for the definition of x, the hydroxide-to-benzoate substitution ratio). While this estimate is very crude, it indicates that the benzoate substitution of the hydroxide ions is by far not complete even at a large excess of benzoic acid used. The water content of MIL-88B(Cr) should be less than 10% due to the

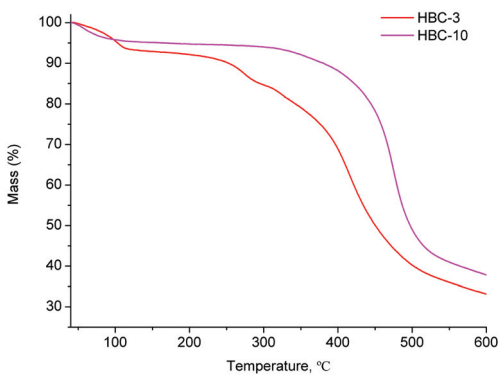

Fig. 4 TGA curves of HBC-3 (nano-MIL-101) and HBC-10 (MIL-88).

much smaller surface area and pore volume,[43] and a value of approx. 4% was observed experimentally.

It has been reported for carboxylate-based MOFs that the use of high concentrations of monocarboxylic acid as modulators[16,30] or higher pH[60] of the synthetic medium could in some cases restrict nucleation and enable the formation of large crystals. Additionally, high concentrations of the modulator could efficiently suppress particle growth.[50,61] In the previous work, we found that at high concentrations of acetic acid, nano-crystals of MIL-101(Cr) could be obtained.[50] In this case, benzoic acid offers a similar effect in a certain concentration range. Nano-MIL-101 forms when a 1 : 1 : 3 ratio of Cr : H_2BDC : HBC is used and the concentration of HBC is 0.6 mol L^{-1}. The concurrence of terephthalate and benzoate ligands and the terminal role of the latter stabilizes the nanocrystals by preventing their growth. This concurrence could also suppress the Ostwald ripening, *i.e.* the growth of the larger particles on account of the smaller ones. Seeds, *viz.* nucleation sites are formed all the time during the synthesis. Effective inhibition of the particle size growth allows reaching of relatively uniform crystallite sizes, *i.e.* obtain a relatively monodisperse product. However, when the concentration of the benzoic acid is increased nearly three-fold with a molar ratio of 1 : 1 : 10 for Cr : H_2BDC : HBC, the stabilization of the MIL-101(Cr) phase does not occur and MIL-88B(Cr) forms straightforwardly. Interestingly, the mechanism of the small particle stabilization also fails in the latter case, *i.e.* benzoic acid demonstrates a much higher influence on the morphology of MIL-101(Cr) compared to MIL-88(Cr).

Experimental section

Materials

Chromium(III) nitrate nonahydrate (AR, 99%, Aladdin), benzene-1,4-dicarboxylic acid (99%, Aladdin), benzoic acid (AR, 99.5+%, Sinopharm chemical reagent Co., Ltd), *N*,*N*-dimethylformamide (DMF, AR, 99.5+%, Sinopharm Chemical Reagent Co., Ltd) and ethanol (AR, 99.7+%, Sinopharm Chemical Reagent Co., Ltd). All chemicals were used as obtained from commercial sources without further purification.

Instrumentation

Powder X-ray diffraction (XRD) measurements were carried out on samples at ambient temperature by using an Ultima IV instrument with a flat sample holder. Simulated PXRD patterns were calculated from single crystal data by the MERCURY 3.0.1 software.[30] Small-angle XRD patterns were obtained on a SmartLab instrument.

Nitrogen physisorption isotherms were measured at 77 K using a Kubo X1000 instrument within a partial pressure, P/P_0, range of 10^{-6}–~1.0. Before measurements, the samples were degassed at 120 °C for 2 h. The BET surface areas were calculated from adsorption isotherm data points in the P/P_0 range of 0.05–0.2.

Thermogravimetric analysis (TGA) was performed on a TGA/DSC1/1100SF instrument at a 10 °C min^{-1} heating rate using aluminum sample holders and nitrogen as a carrier gas.

Scanning electron microscopy (SEM) characterization was performed on a sample made by dropping 15 μL of a dispersion on a silicon substrate and by drying in air. The measurement was done using a Nova NanoSEM230 instrument.

Transmission electron microscopy (TEM) was conducted on a JEM-2100F instrument by dropping a 3 μL suspension of a dispersion onto a carbon-coated Formvar copper grid (300 mesh) followed by drying at room temperature.

Synthesis and purification

A mixture of chromium(III) nitrate nonahydrate ($Cr(NO_3)_3{\cdot}9H_2O$; 1.2 g, 3.0 mmol), benzene-1,4-dicarboxylic acid (H_2BDC; 0.498 g, 3.0 mmol) and benzoic acid (HBC; 0–~3.66 g, 0–~30 mmol) in 15 mL H_2O was transferred to a PTFE/Teflon lined autoclave. The autoclave was sealed, heated for 8 h at 220 °C and cooled afterwards to room temperature at a rate of 25 °C h^{-1}.

The contents of the autoclave were transferred to centrifuge tubes and the supernatant solution was carefully removed after centrifugation. The resulting solid was stirred in DMF (45 mL) and this washing step was concluded by separation of the solid phase by centrifugation. The washings were repeated in DMF (45 mL, 16 h) and ethanol (45 mL for 1 h and 45 mL for 16 h of stirring). After the final isolation, the resulting wet solid was dried in a vacuum oven (120 °C, 12 mbar) for 2 h. Samples B-5, B-8 and B-10 were further activated in air at 120 °C, 250 °C and 350 °C for 12 h, respectively.

Conflicts of interest

There are no conflicts to declare.

Acknowledgements

The work was supported by the National Natural Science Foundation of China (51802094), the Science and Technology Program of Hunan Province, China (2018RS3084), and the Hunan Provincial Natural Science Foundation of China (2018JJ3122). X. Y. thanks the National Key R&D Program of China (2017YFC1103800), the NNSFC (5181101338, U1663225, 51611530672, 21711530705), and the Hubei Provincial Natural Science Foundation of China (2016CFA033). L. Y. thanks the Hunan Provincial Innovation Foundation for Postgraduate (CX2017B679). C. J. thanks the BMBF for grant Optimat 03SF0492C. D. L. thanks the Hunan Provincial Department of Education (No. 17B070) for funding. Y. L. thanks the NNSFC (11872179). T. Z. and I. B. thank Dr Felix Jeremias for fruitful discussions regarding the synthesis of chromium dicarboxylate MOFs.

Notes and references

1 S. R. Batten, N. R. Champness, X.-M. Chen, J. Garcia-Martinez, S. Kitagawa, L. Öhrström, M. O'Keeffe, M. P. Suh and J. Reedijk, *CrystEngComm*, 2012, **14**, 3001–3004.

2 S. R. Batten, N. R. Champness, X.-M. Chen, J. Garcia-Martinez, S. Kitagawa, L. Öhrström, M. O'Keeffe, M. P. Suh and J. Reedijk, *Pure Appl. Chem.*, 2013, **85**, 1715–1724.

3 C. Janiak and J. K. Vieth, *New J. Chem.*, 2010, **34**, 2366–2388.

4 T. Zhao, C. Heering, I. Boldog, K. V. Domasevitch and C. Janiak, *CrystEngComm*, 2017, **19**, 776–780.

5 M. Paik Suh, H. J. Park, T. K. Prasad and D.-W. Lim, *Chem. Rev.*, 2012, **112**, 782–835.

6 Y. Wang, M. Rui and G. Lu, *J. Sep. Sci.*, 2018, **41**, 180–194.

7 B. Zheng, H. Liu, Z. Wang, X. Yu, P. Yi and J. Bai, *CrystEngComm*, 2013, **15**, 3517–3520.

8 C. Xin, H. Zhan, X. Huang, H. Li, N. Zhao, F. Xiao, W. Wei and Y. Sun, *RSC Adv.*, 2015, **5**, 27901–27911.

9 T. Zhao, M. Dong, L. Yang and Y. Liu, *Catalysts*, 2018, **8**, 394.

10 M. Sun, S. Huang, L. Chen, Y. Li, X. Yang, Z. Yuan and B. Su, *Chem. Soc. Rev.*, 2016, **45**, 3479–3563.

11 F. Jeremias, D. Fröhlich, C. Janiak and S. K. Henninger, *RSC Adv.*, 2014, **4**, 24073–24082.

12 C. Orellana-Tavra, S. A. Mercado and D. Fairen-Jimenez, *Adv. Healthcare Mater.*, 2016, **5**, 2261–2270.

13 Y. Zhang, B. Li, H. Ma, L. Zhang, H. Jiang, H. Song, L. Zhang and Y. Luo, *J. Mater. Chem. C*, 2016, **4**, 7294–7301.

14 C. Xin, H. Zhan, X. Huang, H. Li, N. Zhao, F. Xiao, W. Wei and Y. Sun, *RSC Adv.*, 2015, **5**, 27901–27911.

15 J. Sánchez-Laínez, B. Zornoza, Á. Mayoral, Á. Berenguer-Murcia, D. Cazorla-Amorós, C. Télleza and J. Coronas, *J. Mater. Chem. A*, 2015, **3**, 6549–6556.

16 S. Diring, S. Furukawa, Y. Takashima, T. Tsuruoka and S. Kitagawa, *Chem. Mater.*, 2010, **22**, 4531–4538.

17 X. Yang, L. Chen, Y. Li, J. C. Rooke, C. Sanchez and B. Su, *Chem. Soc. Rev.*, 2017, **46**, 481–558.

18 X. Yang, G. Tian, L. Chen, Y. Li, J. C. Rooke, Y. Wei, Z. Liu, Z. Deng, G. V. Tendeloo and B. Su, *Chem. – Eur. J.*, 2011, **17**, 14987–14995.

19 F. Carson, J. Su, A. E. Platero-Prats, W. Wan, Y. Yun, L. Samain and X. Zou, *Cryst. Growth Des.*, 2013, **13**, 5036–5044.

20 S. Bauer, C. Serre, T. Devic, P. Horcajada, J. Marrot, G. Férey and N. Stock, *Inorg. Chem.*, 2008, **47**, 7568–7576.

21 A. Sonnauer, F. Hoffmann, M. Froba, L. Kienle, V. Duppel, M. Thommes, C. Serre, G. Ferey and N. Stock, *Angew. Chem., Int. Ed.*, 2009, **48**, 3791–3794.

22 G. Férey, C. Mellot-Draznieks, C. Serre, F. Millange, J. Dutour, S. Surble and I. Margiolaki, *Science*, 2005, **309**, 2040–2042.

23 K. Leng, Y. Sun, X. Li, S. Sun and W. Xu, *Cryst. Growth Des.*, 2016, **16**, 1168–1171.

24 M. Wickenheisser and C. Janiak, *Microporous Mesoporous Mater.*, 2015, **204**, 242–250.

25 T. Zhao, I. Boldog, C. Janiak and Y. J. Liu, *Chin. J. Inorg. Chem.*, 2017, **33**, 1330–1338.

26 T. Zhao, M. Dong, Y. Zhao and Y. J. Liu, *Prog. Chem.*, 2017, **29**, 1252–1259.

27 S. Bernt, V. Guillerm, C. Serre and N. Stock, *Chem. Commun.*, 2011, **47**, 2838–2840.

28 G. Akiyama, R. Matsuda, H. Sato, A. Hori, M. Takata and S. Kitagawa, *Microporous Mesoporous Mater.*, 2012, **157**, 89–93.

29 P. Horcajada, C. Serre, M. Vallet-Regi, M. Sebban, F. Taulelle and G. Férey, *Angew. Chem., Int. Ed.*, 2006, **45**, 5974–5978.

30 D. M. Jiang, A. D. Burrows and K. J. Edler, *CrystEngComm*, 2011, **13**, 6916–6919.

31 X. Li, Y. Mao, K. Leng, G. Ye, Y. Sun and W. Xu, *Mater. Lett.*, 2017, **197**, 192–195.

32 X. Li, Y. Mao, K. Leng, G. Ye, Y. Sun and W. Xu, *Microporous Mesoporous Mater.*, 2017, **254**, 114–120.

33 C. Serre, C. Mellot-Draznieks, S. Surble, N. Audebrand, Y. Filinchuk and G. Ferey, *Science*, 2007, **315**, 1828–1831.

34 J. He, Y. Zhang, X. Zhang and Y. Huang, *Sci. Rep.*, 2018, **8**, 5159.

35 C. Zhao, Y. Liu and Y. Li, *Anal. Sci.*, 2015, **31**, 1035–1039.

36 C. Gao, H. Zhu, J. Chen and H. Qiu, *Chin. Chem. Lett.*, 2017, **28**, 1006–1012.

37 Y. Zhang, W. Zhang, K. Chen, Q. Yang, N. Hu, Y. Suo and J. Wang, *Sens. Actuators, B*, 2018, **262**, 95–101.

38 P. Horcajada, T. Chalati, C. Serre, B. Gillet, C. Sebrie, T. Baati, J. F. Eubank, D. Heurtaux, P. Clayette, C. Kreuz, J. S. Chang, Y. K. Hwang, V. Marsaud, P. N. Bories, L. Cynober, S. Gil, G. Férey, P. Couvreur and R. Gref, *Nat. Mater.*, 2010, **9**, 172–178.

39 A. C. McKinlay, J. F. Eubank, S. Wuttke, B. Xiao, P. S. Wheatley, P. Bazin, J.-C. Lavalley, M. Daturi, A. Vimont, G. De Weireld, P. Horcajada, C. Serre and R. E. Morris, *Chem. Mater.*, 2013, **25**, 1592–1599.

40 J. He, Y. Zhang, X. Zhang and Y. Huang, *Sci. Rep.*, 2018, **8**, 5159.

41 E. Rahmani and M. Rahmani, *Microporous Mesoporous Mater.*, 2017, **249**, 118–127.

42 C. Serre, F. Millange, S. Surblé and G. Férey, *Angew. Chem., Int. Ed.*, 2004, **43**, 6285–6289.

43 S. Surblé, C. Serre, C. Mellot-Draznieks, F. Millangea and G. Férey, *Chem. Commun.*, 2006, **3**, 284–286.

44 T. Tanasaro, K. Adpakpang, S. Ittisanronnachai, K. Faungnawakij, T. Butburee, S. Wannapaiboon, M. Ogawa and S. Bureekaew, *Cryst. Growth Des.*, 2018, **18**, 16–21.

45 G.-T. Vuong, M.-H. Pham and T.-O. Do, *Dalton Trans.*, 2013, **42**, 550–557.

46 S. Choi, W. Cha, H. Ji, D. Kim, H. J. Lee and M. Oh, *Nanoscale*, 2016, **8**, 16743–16751.

47 T. Shen, J. Luo, S. Zhang and X. Luo, *J. Environ. Chem. Eng.*, 2015, **3**, 1372–1383.

48 J. Zhou, K. Liu, C. Kong and L. Chen, *Bull. Korean Chem. Soc.*, 2013, **34**, 1625–1631.

49 T. Zhao, F. Jeremias, I. Boldog, B. Nguyen, S. K. Henninger and C. Janiak, *Dalton Trans.*, 2015, **44**, 16791–16801.

50 T. Zhao, L. Yang, P. Feng, I. Gruber, C. Janiak and Y. Liu, *Inorg. Chim. Acta*, 2018, **471**, 440–445.

51 E. Bagherzadeh, S. M. Zebarjad and H. R. Madaah Hosseini, *Eur. J. Inorg. Chem.*, 2018, 1–18.

52 T. Rijnaarts, R. Mejia-Ariza, R. J. M. Egberink, W. Vanroosmalen and J. Huskens, *Chem. – Eur. J.*, 2015, **21**, 10296–10301.

53 X. Cai, J. Lin and M. Pang, *Cryst. Growth Des.*, 2016, **16**, 3565–3568.

54 T. Chalati, P. Horcajada, R. Gref, P. Couvreur and C. Serre, *J. Mater. Chem.*, 2011, **21**, 2220–2227.

55 K. Brandenburg, *Diamond (Version 3.2), crystal and molecular structure visualization, Crystal Impact*, K. Brandenburg & H. Putz Gbr, Bonn, Germany, 2007–2012.

56 M. Thommes, K. Kaneko, A. V. Neimark, J. P. Olivier, F. Rodriguez-Reinoso, J. Rouquerol and K. S. W. Sing, *Pure Appl. Chem.*, 2015, **87**, 1051–1069.

57 P. Horcajada, F. Salles, S. Wuttke, T. Devic, D. Heurtaux, G. Maurin, A. Vimont, M. Daturi, O. David, E. Magnier, N. Stock, Y. Filinchuk, D. Popov, C. Riekel, G. Férey and C. Serre, *J. Am. Chem. Soc.*, 2011, **133**, 17839–17847.

58 T. Düren, F. Millange, G. Férey, K. S. Walton and R. Q. Snurr, *J. Phys. Chem. C*, 2007, **111**, 15350–15356.

59 K. S. Walton and R. Q. Snurr, *J. Am. Chem. Soc.*, 2007, **129**, 8552–8556.

60 N. A. Khan, I. J. Kang, H. Y. Seok and S. H. Jhung, *Chem. Eng. J.*, 2011, **166**, 1152–1157.

61 S. Hermes, T. Witte, T. Hikov, D. Zacher, S. Bahnmüller, G. Langstein, K. Huber and R. A. Fischer, *J. Am. Chem. Soc.*, 2007, **129**, 5324–5325.